ADVANCED FUNCTIONAL MATERIALS

Supporting Information

for *Adv. Funct. Mater.*, DOI 10.1002/adfm.202308545

Carrier Trapping Deactivation by Halide Alloying in Formamidinium-Based Lead Iodide Perovskites

*Jesús Jiménez-López, Daniele Cortecchia, E Laine Wong, Giulia Folpini, Antonella Treglia, Ada Lilí Alvarado-Leaños, Chun-Sheng Wu, Andrea Olivati and Annamaria Petrozza**

Supporting Information

Carrier trapping deactivation by halide alloying in formamidinium-based lead iodide perovskites

*Jesús Jiménez-López, Daniele Cortecchia, E Laine Wong, Giulia Folpini, Antonella Treglia, Ada Lilí Alvarado-Leaños, Chun-Sheng Wu, Andrea Olivati, Annamaria Petrozza**

J. Jiménez-López, D. Cortecchia, E L. Wong, G. Folpini, A. Treglia, A.L. Alvarado-Leaños, C-S. Wu, A. Olivati, A. Petrozza
Center for Nano Science and Technology (CNST@PoliMi), Istituto Italiano di Tecnologia (IIT), Milan, 20134, Italy
E-mail: Annamaria.Petrozza@iit.it

D. Cortecchia
Dipartimento di Chimica Industriale "Toso Montanari", Università di Bologna, Bologna, 40136, Italy

A. Treglia, A.L. Alvarado-Leaños, C-S. Wu, A. Olivati
Physics Department, Politecnico di Milano, Milan, 20133, Italy

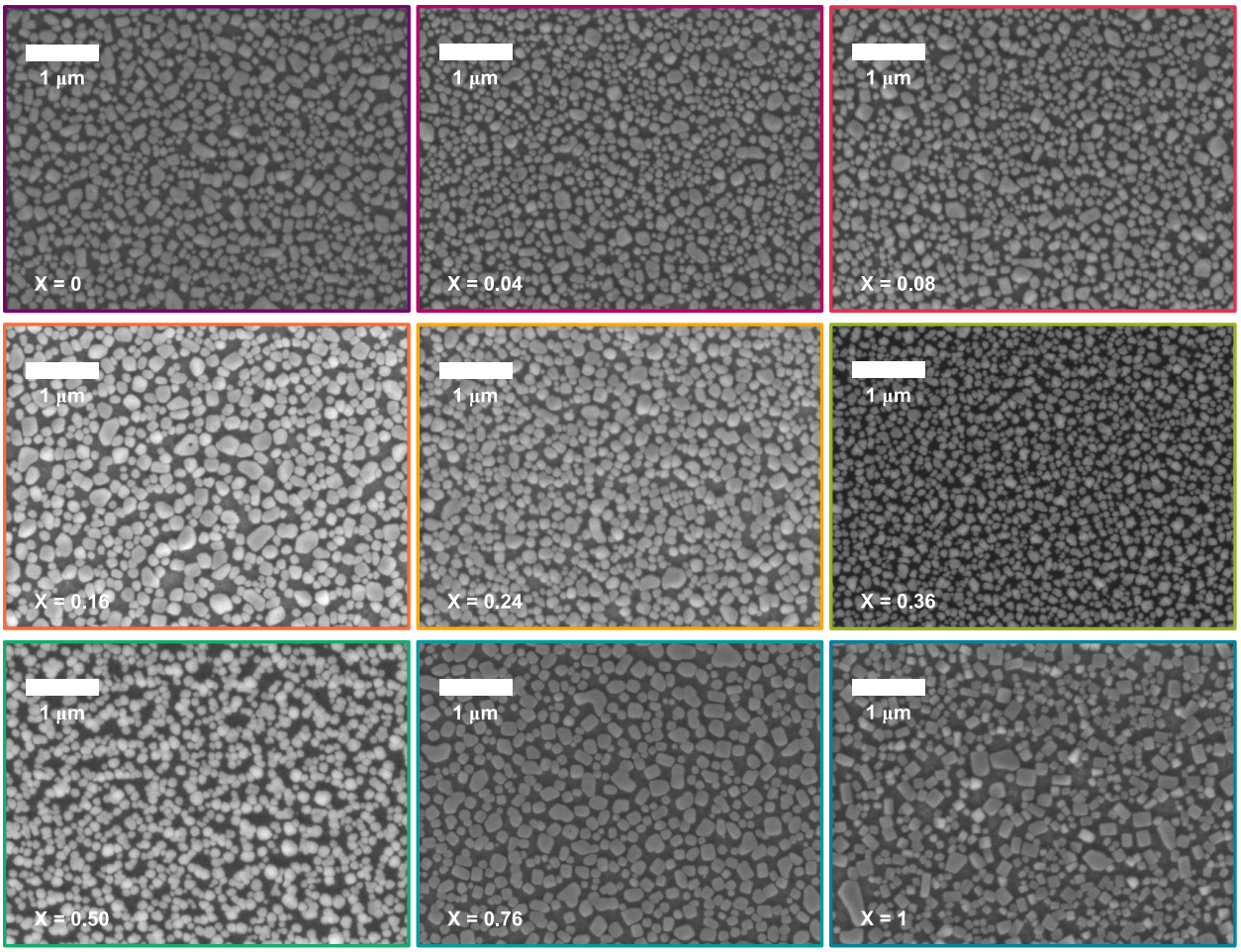

Figure S1. Top-view SEM images of all the $(FAPbI_3)_{1-x}(FAPbBr_3)_x$ compositions. Scale bar is 1 μm.

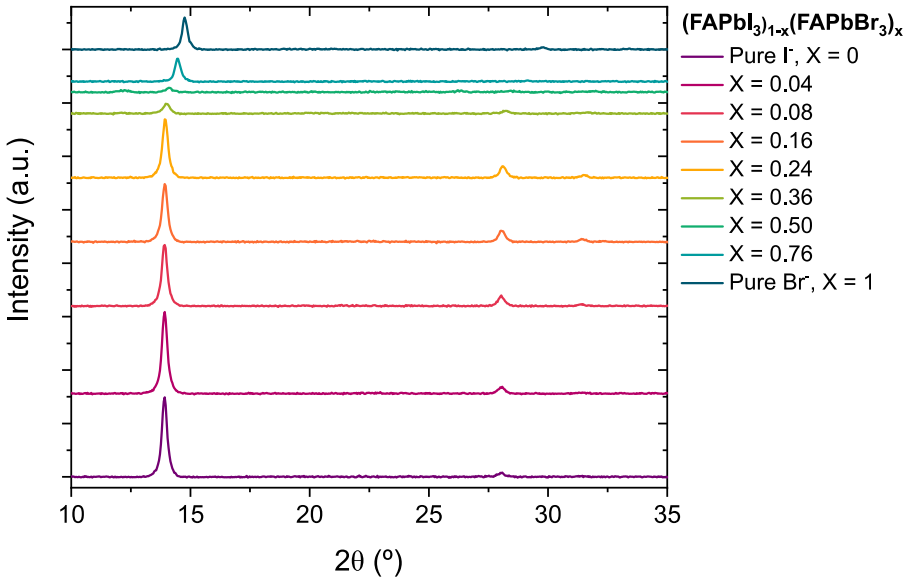

Figure S2. XRD patterns for all the $(FAPbI_3)_{1-x}(FAPbBr_3)_x$ compositions.

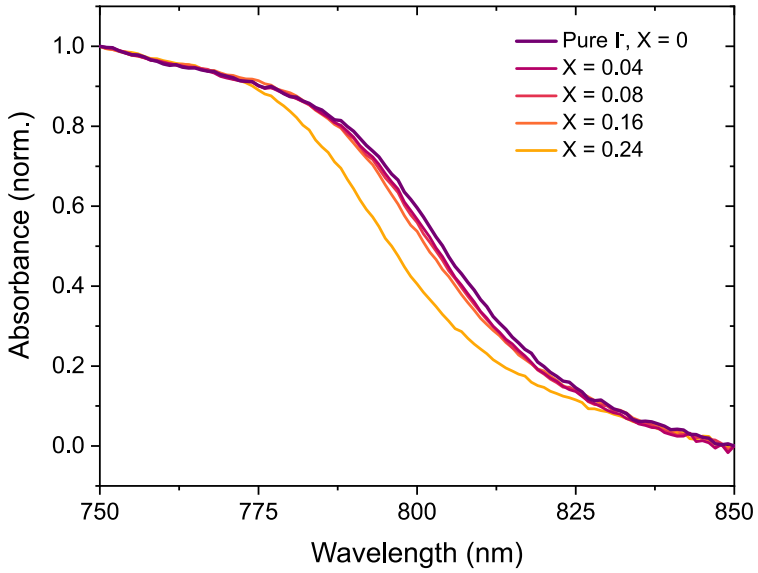

Figure S3. UV-Vis absorption spectra in the region around the band edge for samples X = 0, 0.04, 0.08, 0.16. and 0.24. The spectra were normalized at 750 nm for a better comparison of the band edge shift upon Br incorporation.

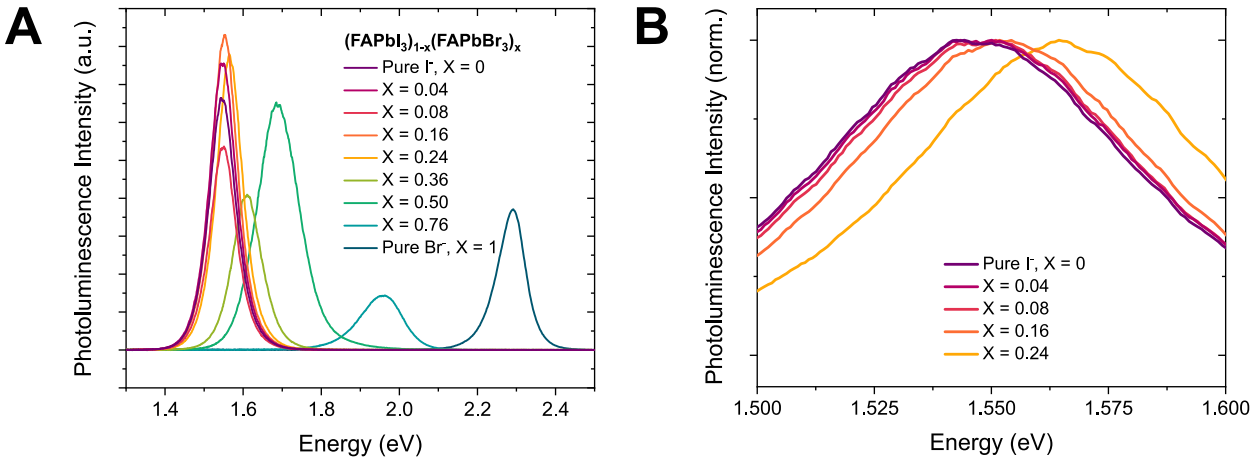

Figure S4. (A) Photoluminescence spectra of all the $(FAPbI_3)_{1-x}(FAPbBr_3)_x$ compositions under a 450 nm excitation. **(B)** Normalized PL spectra for the samples X = 0, 0.04, 0.08, 0.16, and 0.24 for a better appreciation of the PL peak shift to higher energies with Br incorporation.

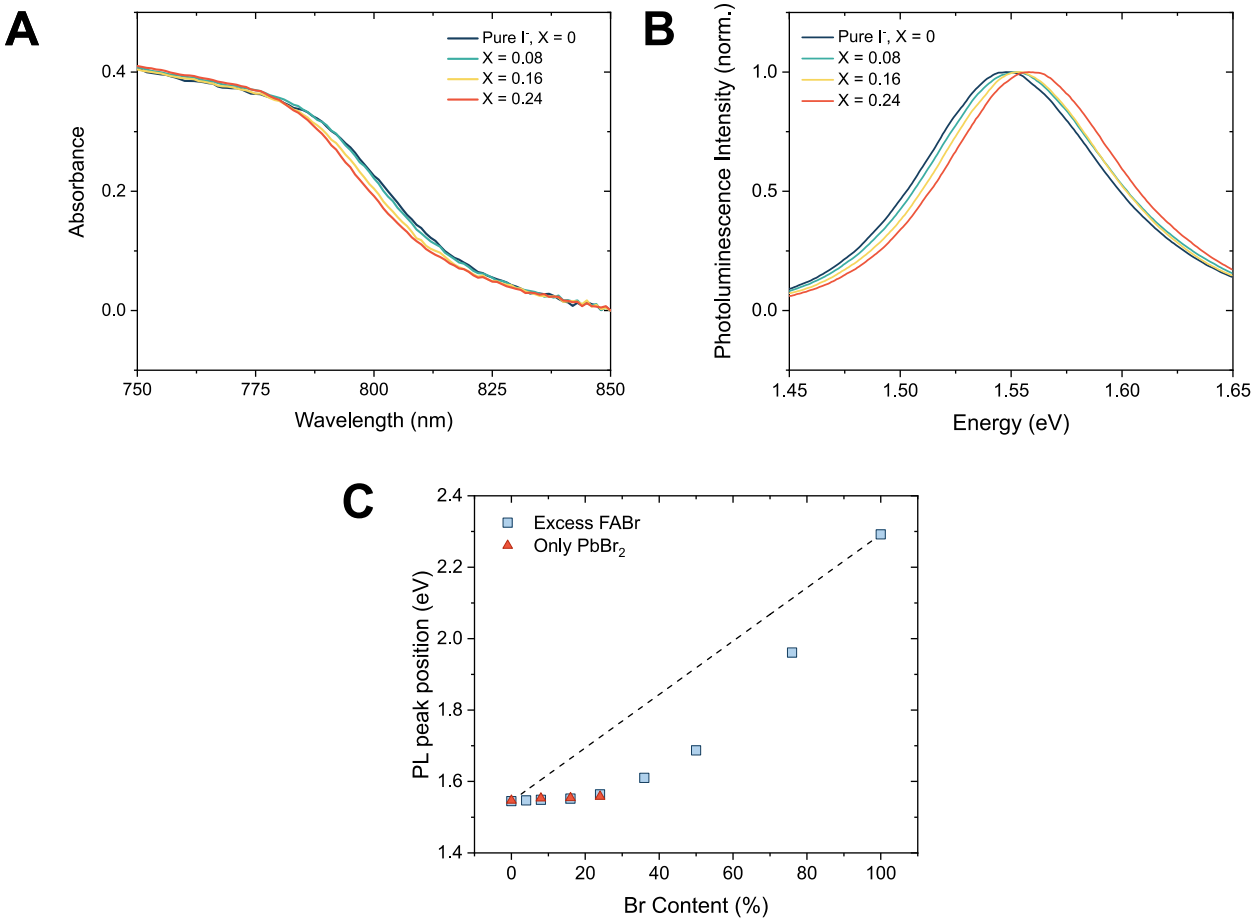

Figure S5. (A) UV-Vis absorption spectra around the band edge of the samples X= 0, 0.08, 0.16, and 0.24, fabricated using $PbBr_2$ as the only Br source. **(B)** Normalized PL spectra of the samples X= 0, 0.08, 0.16, and 0.24, fabricated using $PbBr_2$ as the only Br source. **(C)** Comparison of the

PL peak position of the samples prepared with excess FABr (blue squares) and using $PbBr_2$ as the only Br^- source (orange triangles). The dotted line indicates the linear trend that PL was expected to follow.

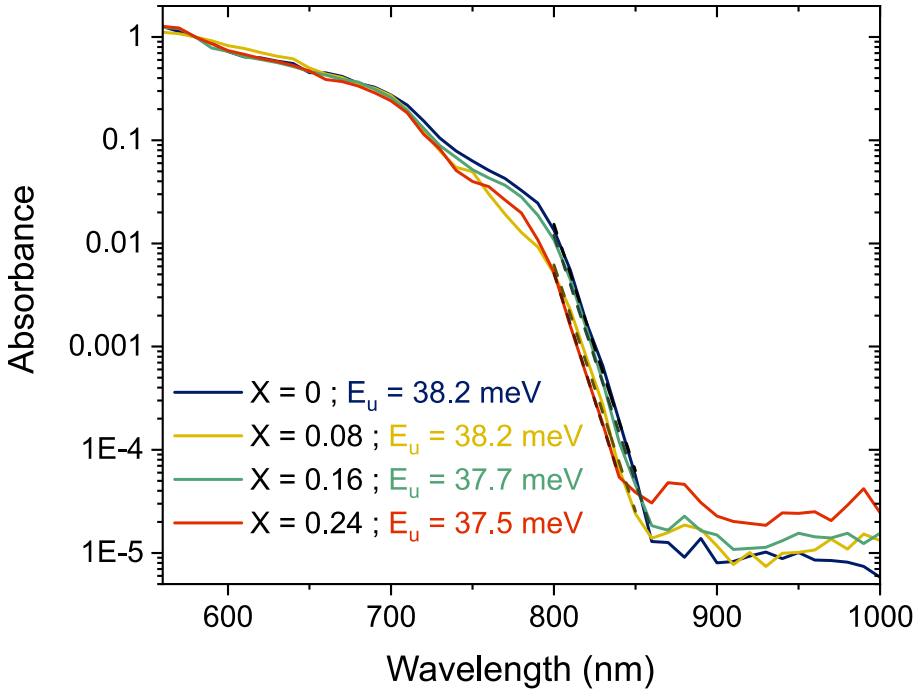

Figure S6. Absorption spectra measured with photothermal deflection spectroscopy. The dotted lines indicate the fittings to obtain the values of Urbach energies (E_U).

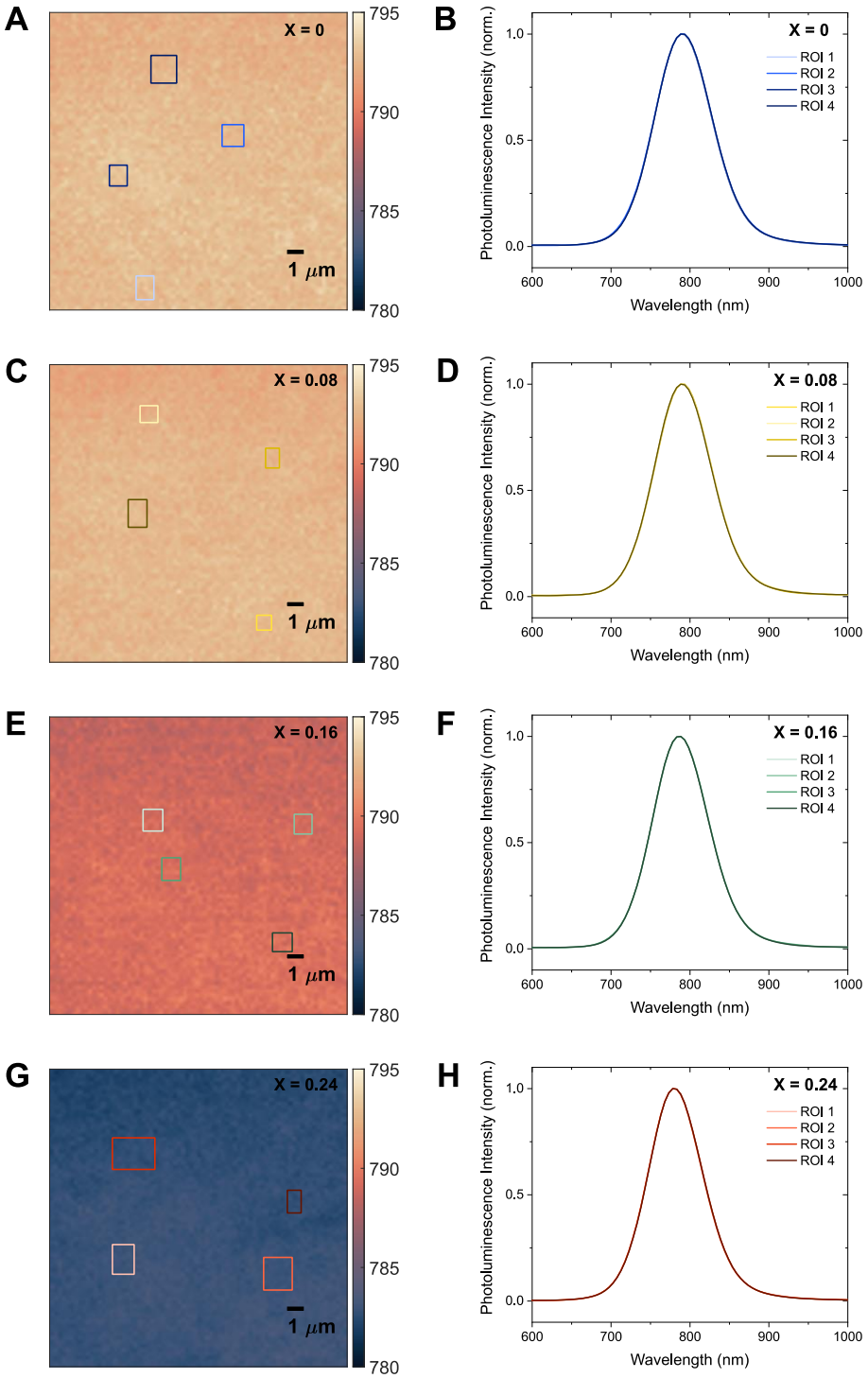

Figure S7. PL mapping showing the homogeneous emission across the film, without the formation of different phases for X = 0 (top left), X = 0.08 (top right), X = 0.16 (bottom left), and X = 0.24 (bottom right). The colorscale represents the maximum of the emission peak in a range from 780 to 795 nm.

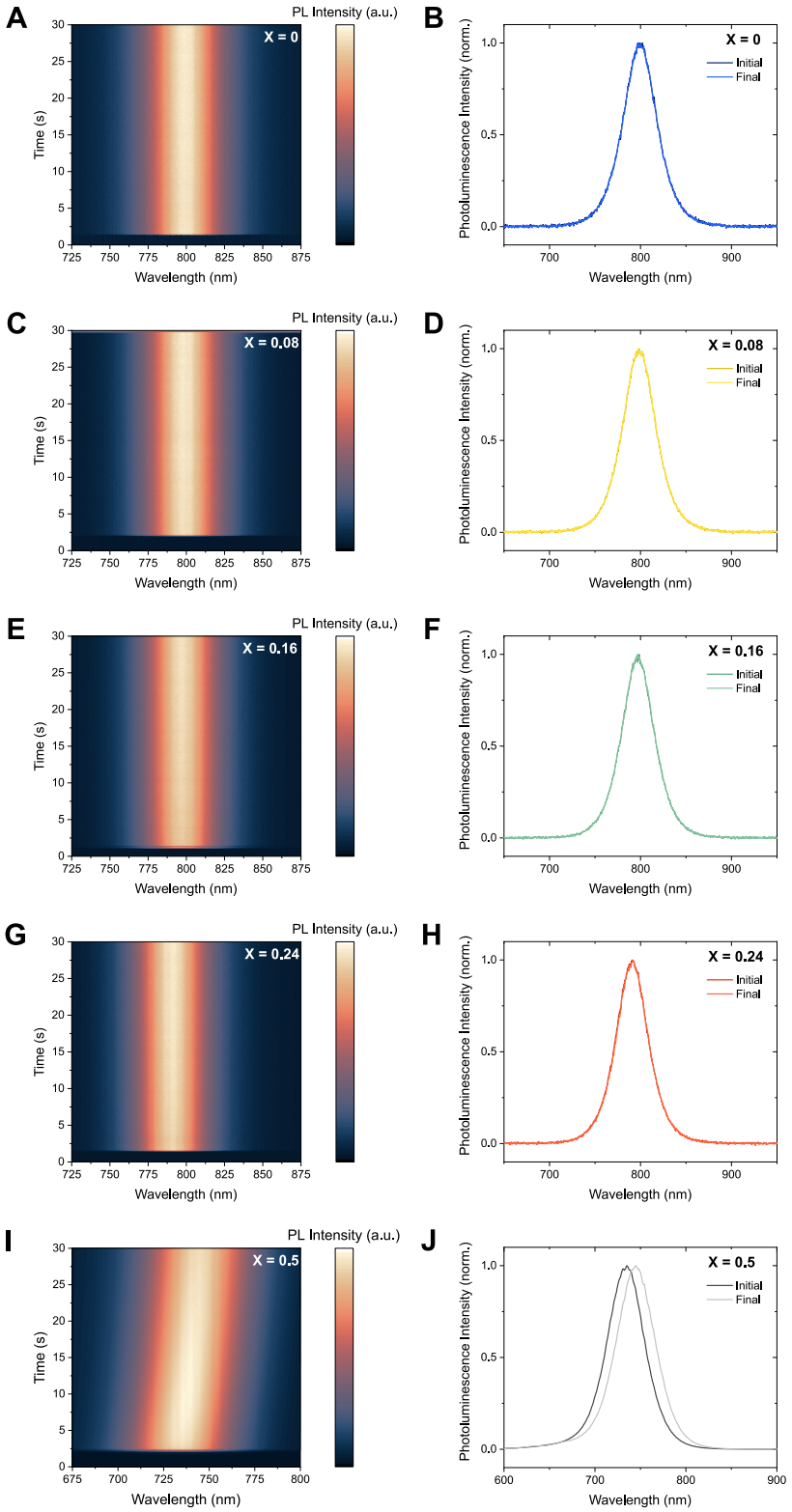

Figure S8. (A)(C)(E)(G)(I) Spectral photoluminescence stability over time and **(B)(D)(F)(H)(J)** extracted initial and final PL spectra for X = 0 **(A)(B)**, X = 0.08 **(C)(D)**, X = 0.16 **(E)(F)**, X = 0.24 **(G)(H)**, and X = 0.5 **(I)(J)**. Samples were excited with a 515 nm excitation wavelength.

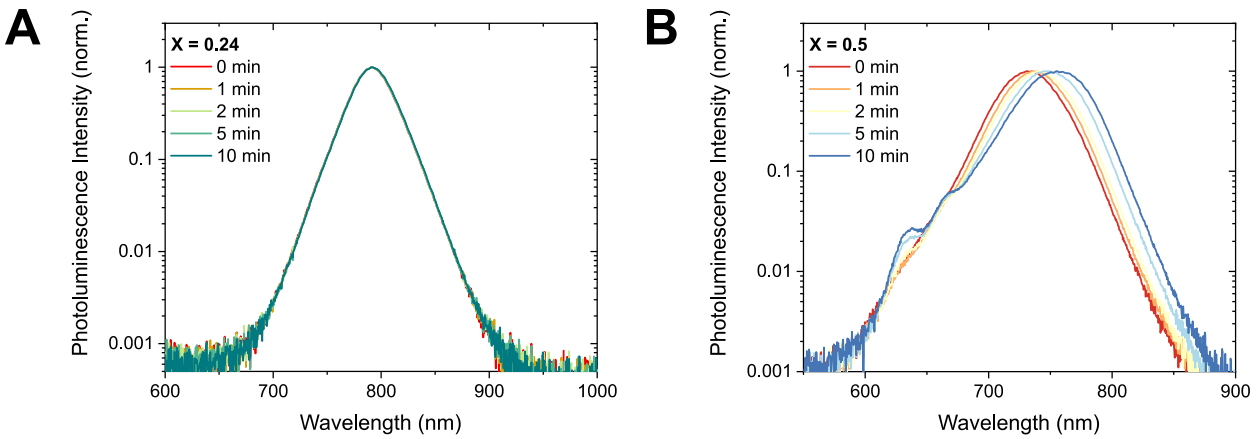

Figure S9. Photoluminescence spectra under continuous illumination with a 450 nm laser over 10 minutes for **(A)** X = 0.24 and **(B)** X = 0.5.

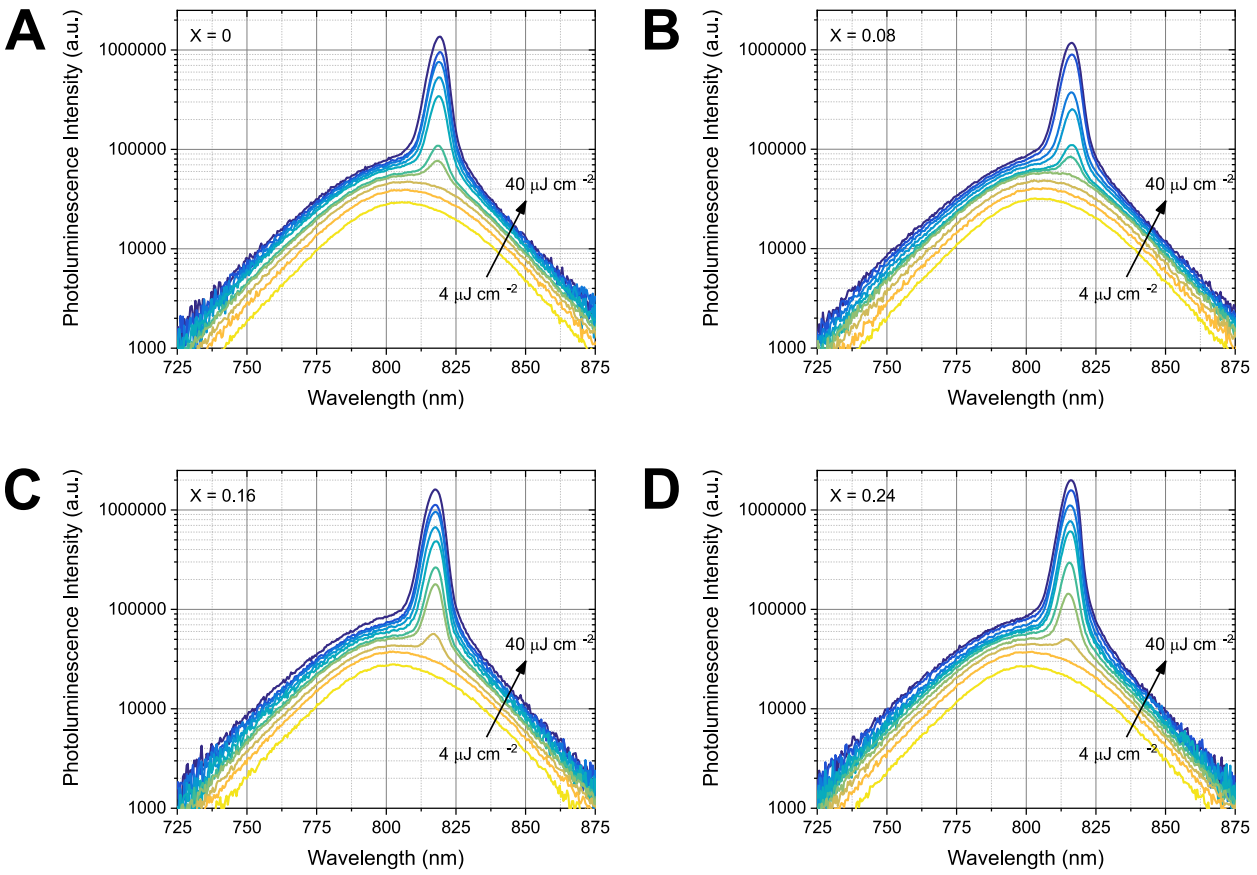

Figure S10. Fluence dependent PL measurements of the samples with compositions $(FAPbI_3)_{1-x}(FAPbBr_3)_x$, where X = 0, 0.08, 0.16, and 0.24, in the fluence range 4-40 μJ cm^{-2}. Samples were excited with a 532 nm laser pulse.

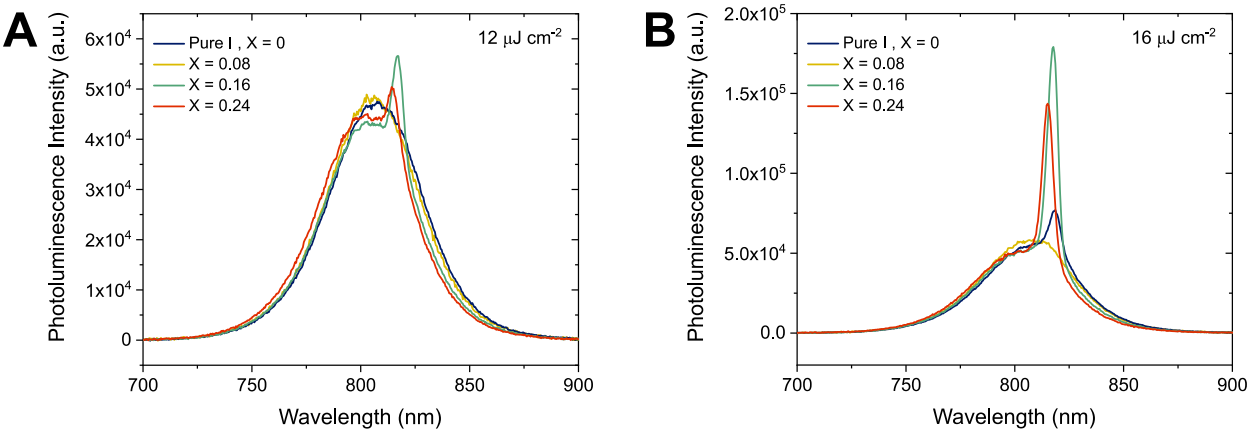

Figure S11. PL measurements of the samples with compositions $(FAPbI_3)_{1-x}(FAPbBr_3)_x$, where X = 0, 0.08, 0.16, and 0.24, using 12 μJ·cm^{-2} **(A)** and 14 μJ·cm^{-2} **(B)** under a 532 nm excitation laser pulse.

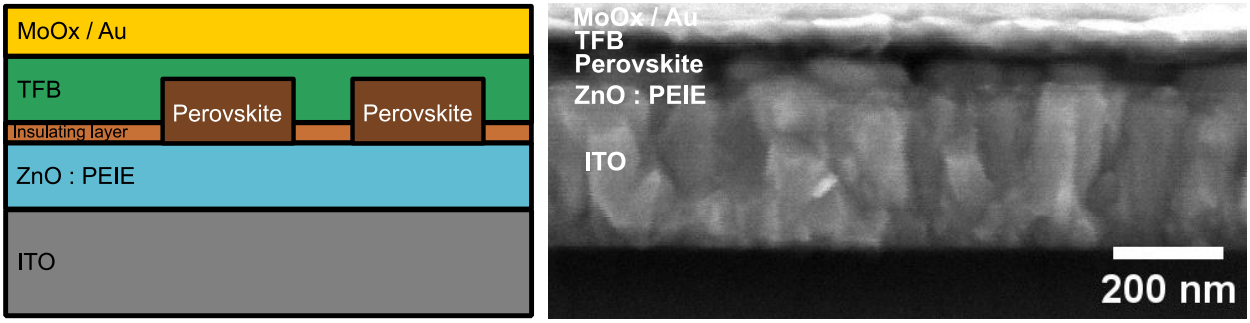

Figure S12. (Left) Scheme showing the PeLED architecture employed. (Right) SEM cross-section image of a device showing the different layers employed.

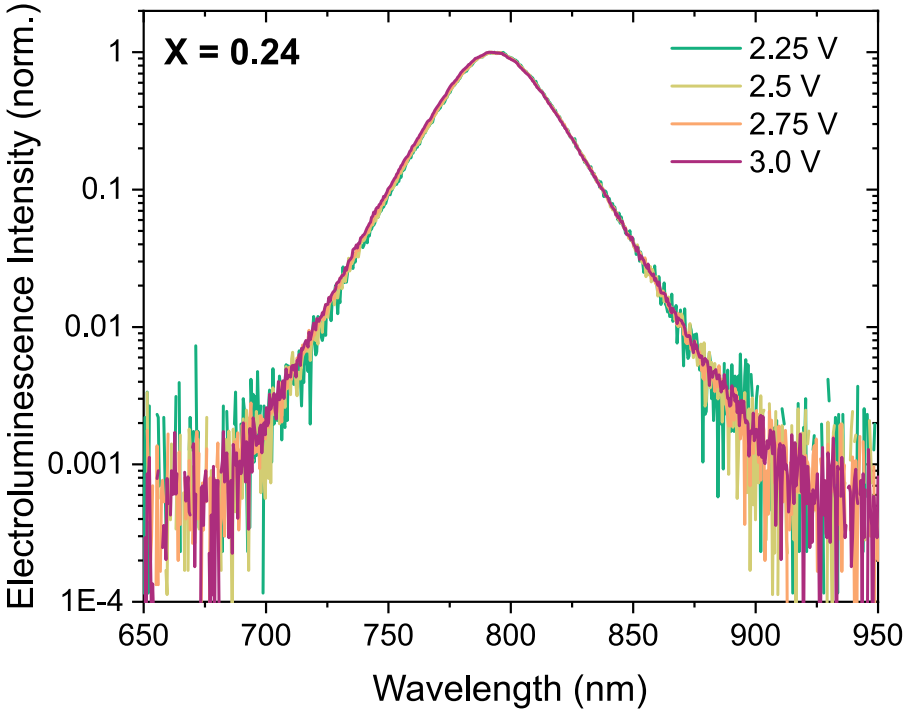

Figure S13. Electroluminescence spectra acquired from 2.25 V to 3 V for X = 0.24.

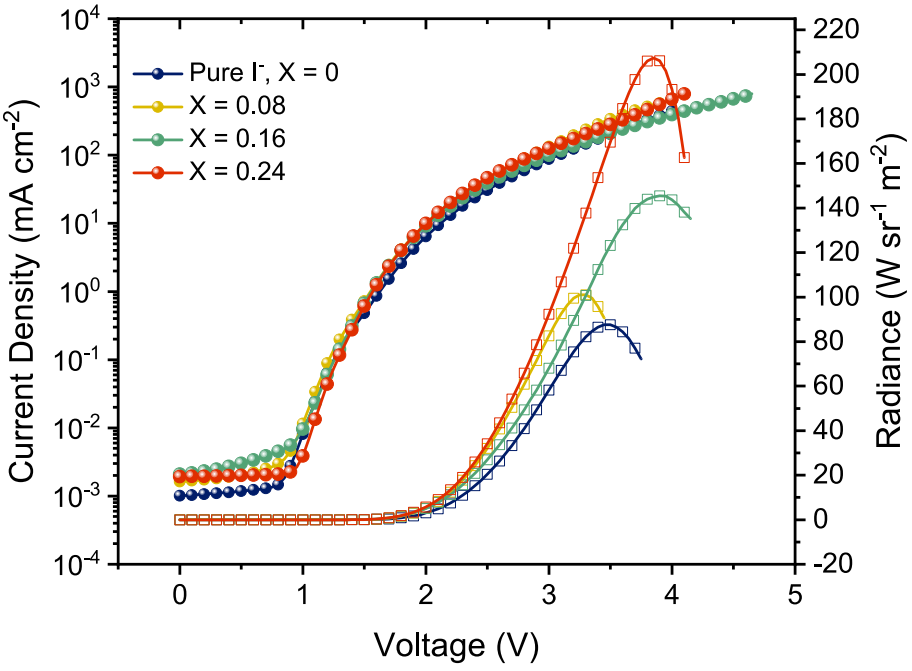

Figure S14. Current density and radiance dependence with the driving voltage.

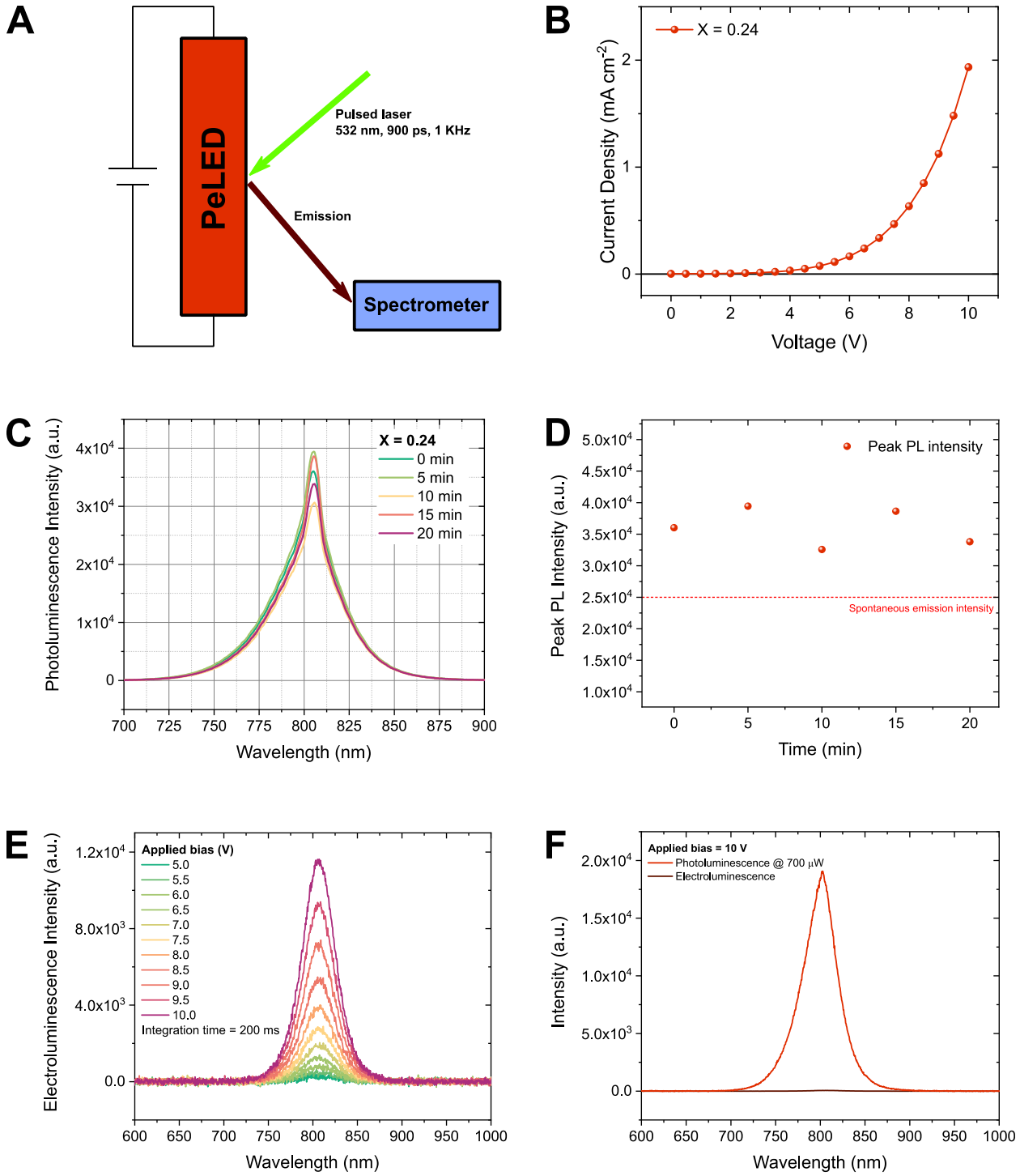

Figure S15. Scheme representing the experimental set-up for the acquisition of ASE under appplied bias **(A)**. Current density-voltage dependence of the PeLED with composition X = 0.24 used for the characterization **(B)**. Emission spectra measured in a X = 0.24 PeLED under continuous laser pumping for 20 minutes **(C)** and the associated peak PL intensity as a function of time **(D)**. Electroluminescence spectra of the PeLED with X = 0.24 composition **(E)**. Comparison between the electroluminescence at V = 10 V and the photoluminescence obtained at the experiment conditions.

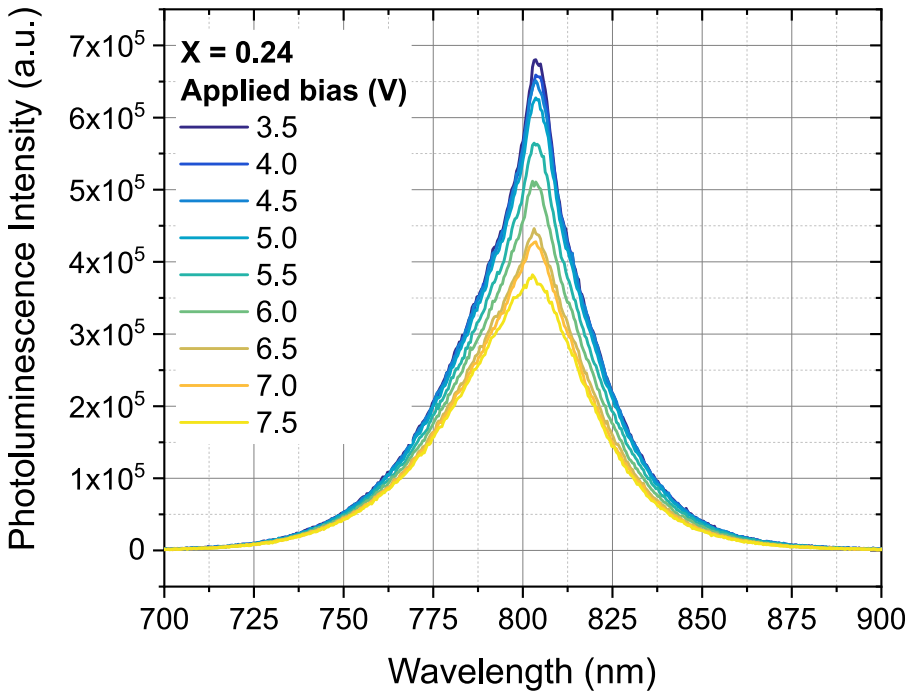

Figure S16. Photoluminescence spectra of X = 0.24 using a LED architecture acquired with an applied positive bias V = 3.5 - 10 V, and using a 532 nm laser pulse as the excitation source. The decrease in emission intensity coincides with the emergence of EL, as observed in Figure S10E.

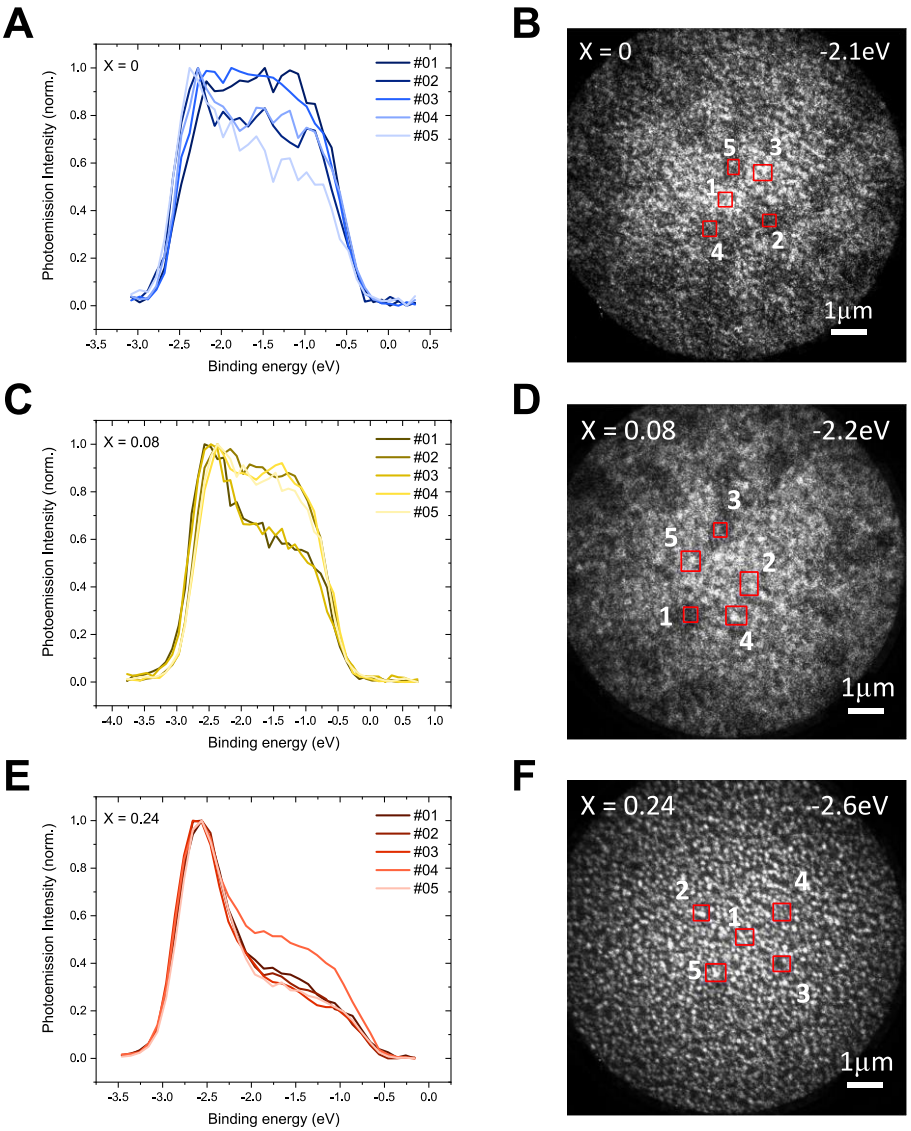

Figure S17. (A)(C)(E) Normalized local photoemission spectra for X = 0 **(A)**, X = 0.08 **(C)**, and X = 0.24 **(E)**. The spectra were acquired in the areas highlighted in red in **(B)**, **(D)**, and **(F)**. **(B)(D)(F)** Spatially resolved PEEM image of X = 0 at a binding energy of -2.1 eV **(B)**, X = 0.08 at a binding energy of -2.2 eV **(D)**, and X = 0.24 at a binding energy of -2.6 eV (right). Scale bar is 1 µm.

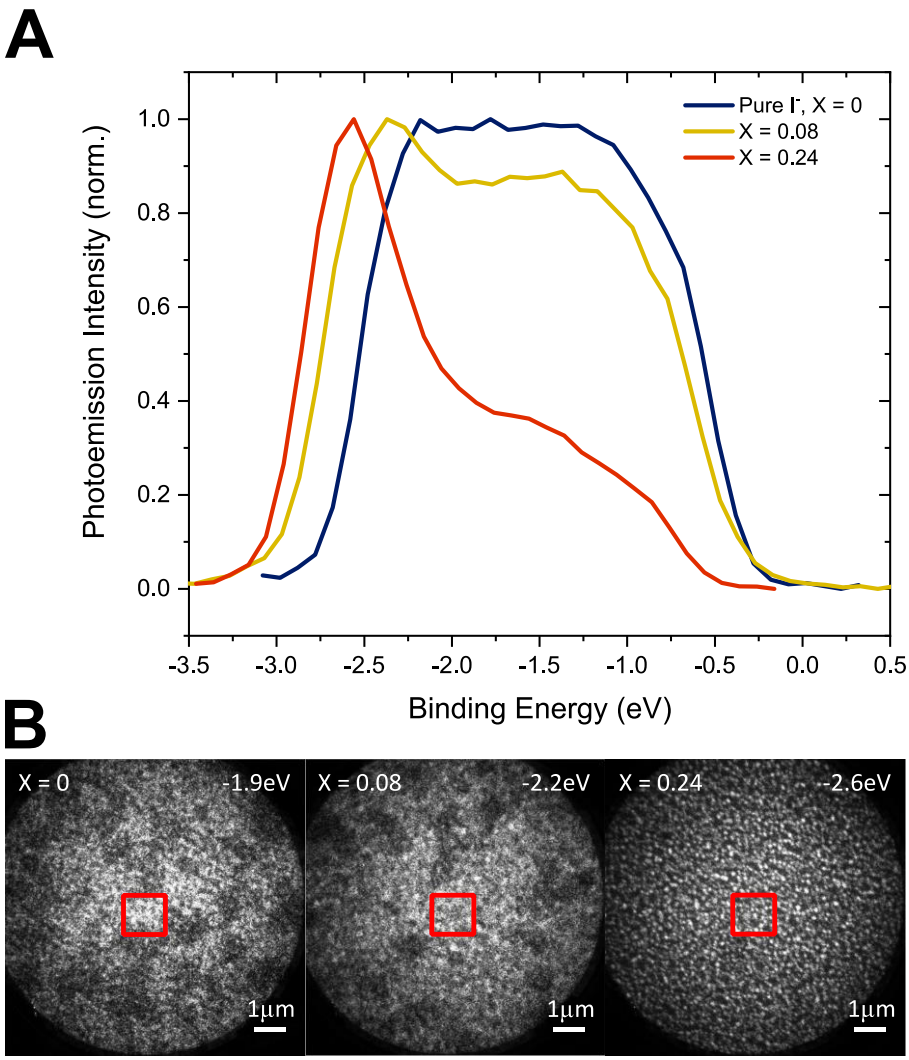

Figure S18. (A) Normalized local photoemission spectra of the regions highlighted in red in **(B)** for X = 0, X = 0.08, and X = 0.24. **(B)** Spatially resolved PEEM image of X = 0 at a binding energy of -1.9 eV (left), X = 0.08 at a binding energy of -2.2 eV (center), and X = 0.24 at a binding energy of -2.6 eV (right). The red squares indicate the regions in which the photoemission spectra was acquired for **(A)**. Scale bar is 1 µm.

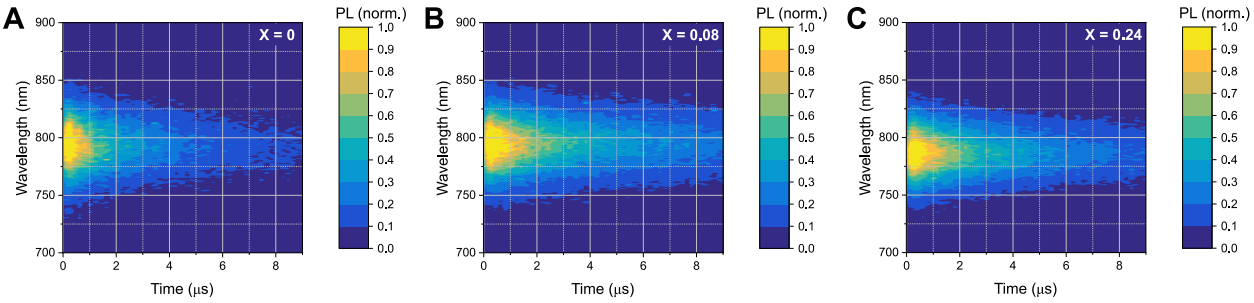

Figure S19. Time resolved photoluminescence maps of X = 0 **(A)**, X = 0.08 **(B)**, and X = 0.24 **(C)** under a 532 nm laser excitation pulse and a $3 \cdot 10^{15}$ cm^{-3} excitation density.

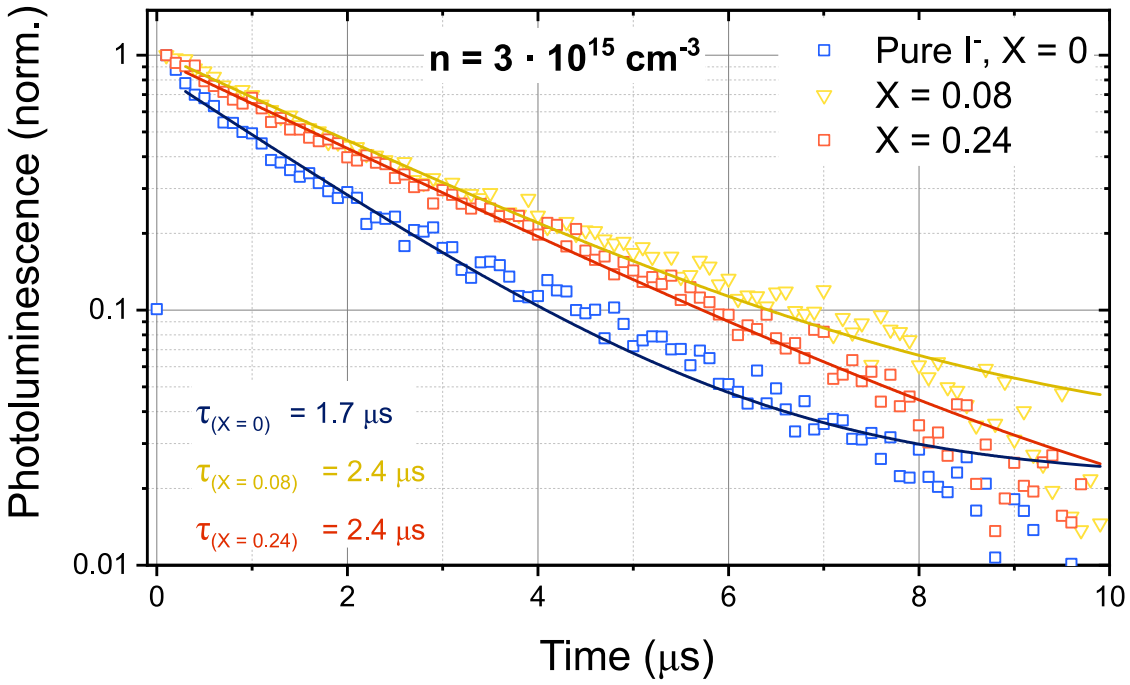

Figure S20. Time resolved photoluminescence decays of X = 0, X = 0.08 and X = 0.24 using a 532 nm excitation and 1 kHz repetition rate, and the monoexponential decay fitting used to extract the PL lifetime.

Supplementary note 1

The photoluminescence energy of mixed-halide perovskite follows Vegard's law (Equation S1):

$$E_{PL}(X) = E_{PL,X=0}(1-X) + E_{PL,X=1}X - bX(1-X) \qquad \text{(S1)}$$

Where E_{PL} is the PL peak energy of the mixed halide composition, $E_{PL,X=0}$ is the PL peak energy of the pure iodide phase, $E_{PL,X=1}$ is the PL peak energy of the pure bromide phase, X is the bromide content and b is the bowing parameter that accounts for deviations from linearity. We obtained b = 0.9, however, one would expect smaller deviations from linearity of the PL peak with the Br^- content.[1]

References

[1] a) M. C. Brennan, A. Ruth, P. V. Kamat, M. Kuno, Trends in Chemistry 2020, 2, 282; b) Y. Chen, S. G. Motti, R. D. J. Oliver, A. D. Wright, H. J. Snaith, M. B. Johnston, L. M. Herz, M. R. Filip, The Journal of Physical Chemistry Letters 2022, 13, 4184; c) Y. Li, Y. Lu, X. Huo, D. Wei, J. Meng, J. Dong, B. Qiao, S. Zhao, Z. Xu, D. Song, RSC Advances 2021, 11, 15688; d) A. Ruth, H. Okrepka, P. Kamat, M. Kuno, The Journal of Physical Chemistry C 2023, 127, 18547.